arXiv:1010.2402v3 [hep-ph] 12 Nov 2010

New physics in $t \to bW$ decay at next-to-leading order in QCD

Jure Drobnak,[1, *] Svjetlana Fajfer,[1, 2, †] and Jernej F. Kamenik[1, ‡]
[1] *J. Stefan Institute, Jamova 39, P. O. Box 3000, 1001 Ljubljana, Slovenia*
[2] *Department of Physics, University of Ljubljana, Jadranska 19, 1000 Ljubljana, Slovenia*

(Dated: November 15, 2010)

We consider contributions of non-standard tbW effective operators to the decay of an unpolarized top quark into a bottom quark and a W gauge boson at next-to-leading order in QCD. We find that $\mathcal{O}_{LR} \equiv \bar{b}_L \sigma_{\mu\nu} t_R W^{\mu\nu}$ contribution to the transverse-plus W helicity fraction ($\mathcal{F}_+$) is significantly enhanced compared to the leading order result at non-vanishing bottom quark mass. Nonetheless, presently the most sensitive observable to direct $\mathcal{O}_{LR}$ contributions is the longitudinal W helicity fraction $\mathcal{F}_L$. In particular, the most recent CDF measurement of $\mathcal{F}_L$ already provides the most stringent upper bound on $\mathcal{O}_{LR}$ contributions, even when compared with indirect bounds from the rare decay $B \to X_s\gamma$.

PACS numbers: 12.38.Bx, 13.88.+e, 14.65.Ha

I. INTRODUCTION

There has been a continuing interest in the measurement of helicity fractions of the W boson from top quark decays by the CDF and D0 collaborations at the Tevatron. Presently, the most precise values are provided by the CDF collaboration [1]

$$\mathcal{F}_L \equiv \Gamma^L/\Gamma = 0.88 \pm 0.11(\text{stat.}) \pm 0.06(\text{sys.})\,, \tag{1a}$$
$$\mathcal{F}_+ \equiv \Gamma^+/\Gamma = -0.15 \pm 0.07(\text{stat.}) \pm 0.06(\text{sys.})\,, \tag{1b}$$

where Γ^L and Γ^+ denote the rates into the longitudinal and transverse-plus polarization state of the W boson, while Γ is the total rate. Note that the central CDF value of $\mathcal{F}_+$ lies outside of the physical region. In the near future, the large $t\bar{t}$ production cross section at the LHC is expected to provide an opportunity to study tbW interactions at the percent level accuracy [2]. It is therefore important to carefully evaluate and understand the implications of such measurements within the Standard Model (SM) and beyond.

In the SM, simple helicity considerations show that $\mathcal{F}_+$ vanishes at the Born term level in the $m_b = 0$ limit. A non-vanishing transverse-plus rate could arise from i) $m_b \neq 0$ effects, ii) $\mathcal{O}(\alpha_s)$ radiative corrections due to gluon emission[1], or from iii) non-SM tbW interactions. The $\mathcal{O}(\alpha_s)$ and the $m_b \neq 0$ corrections to the transverse-plus rate have been shown to occur only at the per-mille level in the SM [4]. Specifically, one obtains

$$\mathcal{F}_L^{\text{SM}} = 0.687(5)\,, \tag{2a}$$
$$\mathcal{F}_+^{\text{SM}} = 0.0017(1)\,. \tag{2b}$$

One could therefore conclude that measured values of $\mathcal{F}_+$ exceeding 0.2% level, would signal the presence of new physics (NP) beyond the SM.

When studying non-standard tbW interactions, constraints from flavor changing neutral current processes involving virtual top quarks within loops play a crucial role. In particular, the inclusive decay $B \to X_s\gamma$ provides stringent bounds on the structure of tbW vertices [5]. One needs to take these constraints into account when evaluating the sensitivity of top decay rate measurements to potential NP contributions.

In the present paper, we study contributions of the non-SM tbW interactions to the W gauge boson helicity fractions in unpolarized top quark decays at next-to-leading order in QCD. We study the impact of QCD radiative corrections on NP constraints as extracted from top quark decay rate measurements and compare those with indirect bounds from inclusive radiative B meson decays.

II. FRAMEWORK

Following [6] we work with a general effective Lagrangian for the tbW interaction, which appears in the presence of new physics (NP) heavy degrees of freedom, integrated out at a scale above the top quark mass (see also [7]). It can be written as

$$\mathcal{L}_{\text{eff}} = \frac{v^2}{\Lambda^2} C_L \mathcal{O}_L + \frac{v}{\Lambda^2} C_{LR} \mathcal{O}_{LR} + (L \leftrightarrow R) + \text{h.c.}\,, \tag{3}$$

with the operators defined as

$$\begin{aligned}\mathcal{O}_L &= \frac{g}{\sqrt{2}} W_\mu \left[\bar{b}_L \gamma^\mu t_L\right], \\ \mathcal{O}_{LR} &= \frac{g}{\sqrt{2}} W_{\mu\nu} \left[\bar{b}_L \sigma^{\mu\nu} t_R\right],\end{aligned} \tag{4}$$

where $q_{R,L} = (1 \pm \gamma_5)q/2$, $\sigma_{\mu\nu} = i[\gamma_\mu, \gamma_\nu]/2$ and g is the weak coupling constant. Furthermore $W_{\mu\nu} = \partial_\mu W_\nu - \partial_\nu W_\mu$ and $v = 246$ GeV is the electroweak condensate.

---

[*] Electronic address:jure.drobnak@ijs.si
[†] Electronic address:svjetlana.fajfer@ijs.si
[‡] Electronic address:jernej.kamenik@ijs.si

[1] Electroweak corrections also contribute, but turn out to be much smaller [3].

Finally, Λ is the effective scale of NP. We adopt a more convenient parameterization

$$\begin{aligned} a_L &= \frac{v^2}{\Lambda^2} C_L = a_L^{\mathrm{SM}} + \delta a_L = V_{tb} + \delta a_L\,, \\ a_R &= \frac{v^2}{\Lambda^2} C_R\,, \qquad b_{LR,RL} = \frac{v m_t}{\Lambda^2} C_{LR,RL}\,, \end{aligned} \tag{5}$$

resulting in the Feynman rule for the effective tbW vertex as shown in Figure 1. We write the complete decay width for $t \to bW$ as a sum of decay widths distinguished by different helicities of the W boson

$$\Gamma_{t\to Wb} = \frac{m_t}{16\pi} \frac{g^2}{2} \sum_i \Gamma^i\,, \tag{6}$$

where $i = L, +, -$ stands for longitudinal, transverse-plus and transverse-minus.

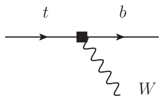

$$= \frac{\mathrm{i}g}{\sqrt{2}} \Big[a_L \gamma^\mu P_L - b_{LR} \frac{2\mathrm{i}\sigma^{\mu\nu}}{m_t} q_\nu P_R + (L \leftrightarrow R) \Big] W_\mu$$

Figure 1: Feynman rule for the effective tbW vertex.

The Γ^i decay rates have already been studied to quite some extent in the existing literature. The tree-level analysis of the effective interactions in (3) has been conducted in Ref. [8]. QCD corrections, however, have been studied only for the chirality conserving operators. Results for a general parametrization can be found in Ref. [9], while SM analysis is given in [10, 11], where $\mathcal{O}(\alpha_s)$ results including $m_b \neq 0$ effects and $\mathcal{O}(\alpha_s^2)$, $m_b = 0$ corrections have been computed. The hard gluon emission corrections are especially important for the observable $\mathcal{F}_+$ since they allow to lift the helicity suppression present at the leading order (LO) in the SM. Helicity suppression in this observable is also exhibited in the presence of the NP operator $\mathcal{O}_{LR}$, which is especially interesting since it is least constrained by indirect bounds coming from the $B \to X_s\gamma$ decay rate [5] and thus has the potential to modify the $t \to bW$ decay properties in an observable way.

III. RESULTS

We compute the $\mathcal{O}(\alpha_s)$ corrections to the polarized rates Γ^i in the $m_b = 0$ limit including both operators given in eq. (4) (and their chirality flipped counterparts). The appropriate Feynman diagrams are presented in Figure 2. We regulate UV and IR divergences by working in $d = 4 + \epsilon$ dimensions. The renormalization procedure closely resembles the one described in [14]. To avoid conceivable problems regarding γ^5 in d-dimensions, we use the prescription of Ref. [12]. To project out the desired helicities of the W boson we use the technique of covariant projectors as described by Fischer et al. in Ref. [4].

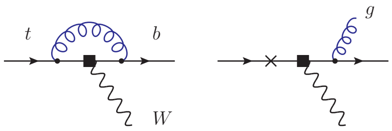

Figure 2: Diagrams for next-to-leading order QCD contributions. Cross marks the additional points from which the gluon can be emitted.

A. The decay rates

In the $m_b = 0$ limit there is no mixing between chirality flipped operators and the decay rates can be written as

$$\begin{aligned} \Gamma^{(L,+,-)} &= |a_L|^2 \Gamma_a^{(L,+,-)} + |b_{LR}|^2 \Gamma_b^{(L,+,-)} \\ &+ 2\mathrm{Re}\{a_L b_{LR}^*\} \Gamma_{ab}^{(L,+,-)} + \langle L \leftrightarrow R, + \leftrightarrow - \rangle\,. \end{aligned} \tag{7}$$

Analytical formulae for $\Gamma^i_{a,b,ab}$ functions are given in the appendix. We have crosschecked Γ^i_a with the corresponding expressions given in [4] and found agreement between the results. The LO ($\mathcal{O}(\alpha_s^0)$) contributions to decay rates $\Gamma^{i,\mathrm{LO}}_{a,b,ab}$ are obtained with a tree-level calculation and are given in Table I. Our results coincide with those given in [8], if the mass m_b is set to zero. The change of $\Gamma^i_{a,b,ab}$ going form LO to next-to-leading order (NLO) in α_s is presented in Table II. Since in the $m_b = 0$ limit $\Gamma^{+,\mathrm{LO}}_{a,b,ab}$ vanish, we use the full m_b dependence of the LO rate when dealing with W transverse-plus helicity. Effectively we neglect the $\mathcal{O}(\alpha_s m_b)$ contributions. In Ref. [10] it has been shown, that these subleading contributions can scale as $\alpha_s(m_b/m_W)^2 \log(m_b/m_t)^2$ leading to a relative effect of a couple of percent compared to the size of $\mathcal{O}(\alpha_s)$ corrections in the $m_b = 0$ limit.

	L	$+$	$-$	unpolarized
$\Gamma_a^{i,\mathrm{LO}}$	$\frac{(1-x^2)^2}{2x^2}$	0	$(1-x^2)^2$	$\frac{(1-x^2)^2(1+2x^2)}{2x^2}$
$\Gamma_b^{i,\mathrm{LO}}$	$2x^2(1-x^2)^2$	0	$4(1-x^2)^2$	$2(1-x^2)^2(2+x^2)$
$\Gamma_{ab}^{i,\mathrm{LO}}$	$(1-x^2)^2$	0	$2(1-x^2)^2$	$3(1-x^2)^2$

Table I: Tree-level decay widths for different W helicities and the their sum, which gives the unpolarized width. All results are in the $m_b = 0$ limit and we have defined $x = m_W/m_t$.

	L	$+$	$-$
$\Gamma_a^{i,\mathrm{NLO}}/\Gamma_a^{i,\mathrm{LO}}$	0.90	3.50	0.93
$\Gamma_b^{i,\mathrm{NLO}}/\Gamma_b^{i,\mathrm{LO}}$	0.96	4.71	0.91
$\Gamma_{ab}^{i,\mathrm{NLO}}/\Gamma_{ab}^{i,\mathrm{LO}}$	0.93	3.75	0.92

Table II: Numerical values for $\Gamma^{\mathrm{NLO}}/\Gamma^{\mathrm{LO}}$ with the following input parameters $m_t = 173$ GeV, $m_W = 80.4$ GeV, $\alpha_s(m_t) = 0.108$. Scale μ appearing in NLO expressions is set to $\mu = m_t$. In addition $m_b = 4.8$ GeV. These values are used throughout the paper for all numerical analysis.

B. Effects on $\mathcal{F}_+$

We have analyzed the effects on $\mathcal{F}_+$ when going from LO to NLO in QCD. Assuming the NP coupling parameters to be real, we consider contributions of a single NP operator at a time. Present 95% C.L. constrains on $\delta a_L, a_R, b_{LR}, b_{RL}$ come from the weak radiative B meson decays ($b \to s\gamma$) analyzed in Ref. [5]. Translated to our definition of parameters these bounds read

$$\begin{aligned} &-0.13 \le \delta a_L \le 0.03\,, -0.0007 \le a_R \le 0.0025\,, \\ &-0.61 \le b_{LR} \le 0.16\,, -0.0004 \le b_{RL} \le 0.0016\,. \end{aligned} \tag{8}$$

Compared with others, constraints on b_{LR} are considerably looser. We present the effect of b_{LR} on $\mathcal{F}_+$ in Figure 3. We see that the the increase is substantial when going to NLO in QCD, but still leaves $\mathcal{F}_+$ at the $1-2$ per-mille level. We summarize the effects of the other NP operators on $\mathcal{F}_+$ in Table III. Nonstandard value of a_L does not effect the different W helicity branching fractions which are the same as in the SM. The dependence of $\mathcal{F}_+$ on non-zero values of a_R and b_{RL} in the $b \to s\gamma$ allowed region is mild, reaching a maximum at the lowest allowed values of a_R and b_{RL}. We observe that for these NP contributions, $b \to s\gamma$ already constrains the value of $\mathcal{F}_+$ to be within 2% of the SM prediction.

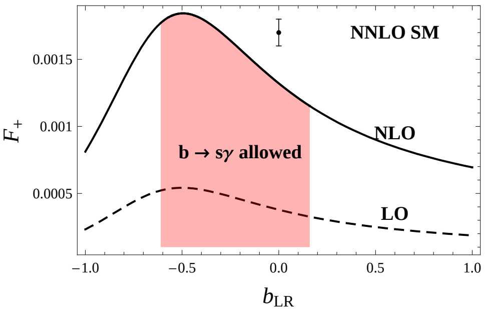

Figure 3: Value of $\mathcal{F}_+$ as a function of b_{LR} (other NP coefficients being set to zero). Red band shows the allowed interval for b_{LR} as given in Ref. [5]. Dashed line coresponds to LO results at $m_b \neq 0$, while the solid line represents the $\mathcal{O}(\alpha_s)$ results. We also present the SM $\mathcal{O}(\alpha_s^2)$ (NNLO) value given in eq. (2b).

	SM (δa_L)	a_R	b_{RL}
$\mathcal{F}_+^{\rm NLO}/\mathcal{F}_+^{\rm LO}$	3.49	3.40	3.38
$\mathcal{F}_+^{\rm NLO}/10^{-3}$	1.32	1.34	1.34

Table III: Maximum allowed effects on $\mathcal{F}_+$ due to non-zero values of a_R and b_{RL} at $\mathcal{O}(\alpha_f)$.

C. Effects on $\mathcal{F}_L$

Analyzing a single real NP operator contribution at the time, leading QCD corrections decrease $\mathcal{F}_L$ by approximately 1% in all cases. Possible effects of a_R and b_{RL} are again severely constrained by $b \to s\gamma$. On the other hand, we find that the most recent CDF measurement of $\mathcal{F}_L$ in eq. (1a) already allows to put competitive bounds on b_{LR} compared to the indirect constraints given in eq. (8). We plot the dependence of $\mathcal{F}_L$ on b_{LR} in Figure 4. A new 95% C.L. upper bound is found to be

$$b_{LR} < 0.09\,, \quad 95\% \text{ C.L.}\,. \tag{9}$$

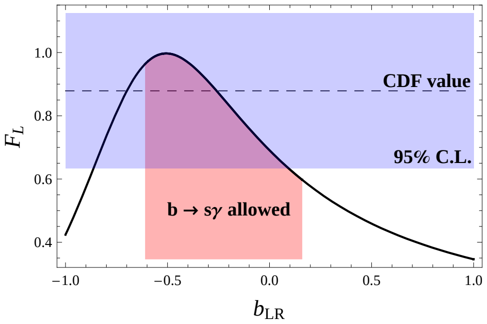

Figure 4: Value of $\mathcal{F}_L$ as a function of b_{LR} (other NP coefficients being set to zero). Red band shows the allowed interval for b_{LR} as given in Ref. [5]. We also present the CDF values given in eq. (1a).

IV. CONCLUSIONS

We have analyzed the decay of an unpolarized top quark to a bottom quark and a polarized W boson as mediated by the most general effective tbW vertex at $\mathcal{O}(\alpha_s)$. We have shown, that within this approach the helicity fraction $\mathcal{F}_+$ can reach maximum values of the order of 2 per-mille in the presence of a non-SM effective operator $\mathcal{O}_{LR}$. Leading QCD effects increase the contributions of $\mathcal{O}_{LR}$ substantially owing to the helicity suppression of the LO result, while other considered NP effective operator contributions are much less affected. Indirect constraints coming from the $B \to X_s\gamma$ decay rate already severely restrict the contributions of these NP operators. In particular, considering only real contributions of a single NP operator at a time, all considered operators except $\mathcal{O}_{LR}$ are constrained to yield $\mathcal{F}_+$ within 2% of the SM prediction. Even in the presence of the much less constrained $\mathcal{O}_{LR}$ contributions, a potential determination of $\mathcal{F}_+$ significantly deviating from the SM prediction, at the projected sensitivity of the LHC experiments [2], could not be explained within such framework. Based on the existing SM calculations of higher order QCD and electroweak corrections [3, 11], we do not expect such corrections to significantly affect our conclusions.

Finally, we have set a new 95% C.L. upper bound on the b_{LR} contributions given in eq. (9), lowering the previous indirect bound coming from $B \to X_s\gamma$ decay by 44%. With increased precision of the $\mathcal{F}_L$ measurements at the

Tevatron and the LHC this bound (as well as the lower bound on the same coupling) is expected to be further significantly improved in the near future.

Acknowledgments

This work is supported in part by the European Commission RTN network, Contract No. MRTN-CT-2006-035482 (FLAVIAnet) and by the Slovenian Research Agency.

[1] T. Aaltonen *et al.* [The CDF Collaboration], Phys. Rev. Lett. **105** (2010) 042002 [arXiv:1003.0224 [hep-ex]].

[2] J. A. Aguilar-Saavedra, J. Carvalho, N. F. Castro, A. Onofre and F. Veloso, Eur. Phys. J. C **53** (2008) 689 [arXiv:0705.3041 [hep-ph]].

[3] H. S. Do, S. Groote, J. G. Körner and M. C. Mauser, Phys. Rev. D **67** (2003) 091501 [arXiv:hep-ph/0209185].

[4] M. Fischer, S. Groote, J. G. Körner and M. C. Mauser, Phys. Rev. D **63** (2001) 031501 [arXiv:hep-ph/0011075].

[5] B. Grzadkowski and M. Misiak, Phys. Rev. D **78** (2008) 077501 [arXiv:0802.1413 [hep-ph]].

[6] J. A. Aguilar-Saavedra, Nucl. Phys. B **812** (2009) 181 [arXiv:0811.3842 [hep-ph]].

[7] C. Zhang and S. Willenbrock, arXiv:1008.3155 [hep-ph]; arXiv:1008.3869 [hep-ph].

[8] J. A. Aguilar-Saavedra, J. Carvalho, N. F. Castro, F. Veloso and A. Onofre, Eur. Phys. J. C **50** (2007) 519 [arXiv:hep-ph/0605190].

[9] W. Bernreuther, M. Fuecker and Y. Umeda, Phys. Lett. B **582** (2004) 32 [arXiv:hep-ph/0308296].

[10] M. Fischer, S. Groote, J. G. Körner and M. C. Mauser, Phys. Rev. D **65** (2002) 054036 [arXiv:hep-ph/0101322].

[11] A. Czarnecki, J. G. Körner and J. H. Piclum, Phys. Rev. D **81** (2010) 111503 [arXiv:1005.2625 [hep-ph]].

[12] S. A. Larin, Phys. Lett. B **303**, 113 (1993) [arXiv:hep-ph/9302240].

[13] J. Drobnak, S. Fajfer and J. F. Kamenik, Phys. Rev. Lett. **104** (2010) 252001 [arXiv:1004.0620 [hep-ph]].

[14] J. Drobnak, S. Fajfer and J. F. Kamenik, Phys. Rev. D **82** (2010) 073016 [arXiv:1007.2551 [hep-ph]].

Appendix A: Analytical Formulae

In this appendix we present analytical formulae for all nine $\Gamma^{L,+,-}_{a,b,ab}$ appearing in eq. (7) to $\mathcal{O}(\alpha_s)$ order and in the $m_b = 0$ limit. Here μ is the arbitrary scale, remnant of operator renormalization, $x = m_W/m_t$ and $C_F = 4/3$. For the computation of $\mathcal{F}_i$, we have also used the $\Gamma_{a,b,ab}$, summed over the three W helicity states. We omit these expressions here, as they coincide with the analoge formulae given in [13, 14] obtained in the context of $t \to cZ$ decays.

1. Longitudinal polarization

$$\begin{aligned}
\Gamma^L_a &= \frac{(1-x^2)^2}{2x^2} + \frac{\alpha_s}{4\pi}C_F\Bigg[\frac{(1-x^2)(5+47x^2-4x^4)}{2x^2} - \frac{2\pi^2}{3}\frac{1+5x^2+2x^4}{x^2} - \frac{3(1-x^2)^2}{x^2}\log(1-x^2) \\
&- \frac{2(1-x)^2(2-x+6x^2+x^3)}{x^2}\log(x)\log(1-x) - \frac{2(1+x)^2(2+x+6x^2-x^3)}{x^2}\log(x)\log(1+x) \\
&- \frac{2(1-x)^2(4+3x+8x^2+x^3)}{x^2}\mathrm{Li}_2(x) - \frac{2(1+x)^2(4-3x+8x^2-x^3)}{x^2}\mathrm{Li}_2(-x) + 16(1+2x^2)\log(x)\Bigg],
\end{aligned} \tag{A1}$$

$$\begin{aligned}
\Gamma^L_b &= 2x^2(1-x^2)^2 + \frac{\alpha_s}{4\pi}C_F\Bigg[-2x^2(1-x^2)(21-x^2) + \frac{2\pi^2}{3}4x^2(1+x^2)(3-x^2) + 4x^2(1-x^2)^2\log\left(\frac{m_t^2}{\mu^2}\right) \\
&- 16x^2(3+3x^2-x^4)\log(x) - 4(1-x^2)^2(2+x^2)\log(1-x^2) - 8x(1-x)^2(3+3x^2+2x^3)\log(x)\log(1-x) \\
&+ 8x(1+x)^2(3+3x^2-2x^3)\log(x)\log(1+x) - 8x(1-x)^2(3+2x+7x^2+4x^3)\mathrm{Li}_2(x) \\
&+ 8x(1+x)^2(3-2x+7x^2-4x^3)\mathrm{Li}_2(-x)\Bigg],
\end{aligned} \tag{A2}$$

$$\begin{aligned}
\Gamma^L_{ab} &= (1-x^2)^2 + \frac{\alpha_s}{4\pi}C_F\Bigg[-(1-x^2)(1+11x^2) - \frac{2\pi^2}{3}(1-7x^2+2x^4) + (1-x^2)^2\log\left(\frac{m_t^2}{\mu^2}\right) \\
&- \frac{2(1-x^2)^2(1+2x^2)}{x^2}\log(1-x^2) - 4x^2(7-x^2)\log(x) - 4(1-x)^2(1+5x+2x^2)\log(x)\log(1-x) \\
&- 4(1+x)^2(1-5x+2x^2)\log(x)\log(1+x) - 4(1-x)^2(3+9x+4x^2)\mathrm{Li}_2(x) - 4(1+x)^2(3-9x+4x^2)\mathrm{Li}_2(-x)\Bigg].
\end{aligned} \tag{A3}$$

2. Transverse-plus polarization

$$\begin{aligned}
\Gamma^+_a &= \frac{\alpha_s}{4\pi}C_F\Bigg[-\frac{1}{2}(1-x)(25+5x+9x^2+x^3) + \frac{\pi^2}{3}(7+6x^2-2x^4) - 2(5-7x^2+2x^4)\log(1+x) \\
&- 2(5+7x^2-2x^4)\log(x) - \frac{(1-x)^2(5+7x^2+4x^3)}{x}\log(x)\log(1-x) - \frac{(1-x)^2(5+7x^2+4x^3)}{x}\mathrm{Li}_2(x) \\
&+ \frac{(1+x)^2(5+7x^2-4x^3)}{x}\log(x)\log(1+x) + \frac{5+10x+12x^2+30x^3-x^4-12x^5}{x}\mathrm{Li}_2(-x)\Bigg],
\end{aligned} \tag{A4}$$

$$\begin{aligned}
\Gamma^+_b &= \frac{\alpha_s}{4\pi}C_F\Bigg[\frac{4}{3}x(1-x)(30+3x+7x^2-2x^3-2x^4) - 4\pi^2x^4 - 8(5-9x^2+4x^4)\log(1+x) + 8x^2(1+5x^2)\log(x) \\
&- 4(1-x)^2(4+5x+6x^2+x^3)\log(x)\log(1-x) - 4(1+x)^2(4-5x+6x^2-x^3)\log(x)\log(1+x) \\
&- 4(1-x)^2(4+5x+6x^2+x^3)\mathrm{Li}_2(x) - 4(4+3x-16x^2+6x^3+16x^4-x^5)\mathrm{Li}_2(-x)\Bigg],
\end{aligned} \tag{A5}$$

$$\begin{aligned}
\Gamma^+_{ab} &= \frac{\alpha_s}{4\pi}C_F\Bigg[2x(1-x)(15-11x) + \frac{2\pi^2}{3}x^2(5-2x^2) - 2(13-16x^2+3x^4)\log(1+x) + 2x^2(1+3x^2)\log(x) \\
&- 2(1-x)^2(5+7x+4x^2)\log(x)\log(1-x) - 2(1+x)^2(5-7x+4x^2)\log(x)\log(1+x) \\
&- 2(1-x)^2(5+7x+4x^2)\mathrm{Li}_2(x) - 2(3+3x-31x^2+x^3+12x^4)\mathrm{Li}_2(-x)\Bigg].
\end{aligned} \tag{A6}$$

3. Transverse-minus polarization

$$\begin{aligned}
\Gamma_a^- \;=&\; (1-x^2)^2 + \frac{\alpha_s}{4\pi} C_F \Bigg[-\frac{1}{2}(1-x)(13+33x-7x^2+x^3) + \frac{\pi^2}{3}(3+4x^2-2x^4) - 2(5+7x^2-2x^4)\log(x) \\
-&\; \frac{2(1-x^2)^2(1+2x^2)}{x^2}\log(1-x) - \frac{2(1-x^2)(1-4x^2)}{x^2}\log(1+x) - \frac{(1-x)^2(5+7x^2+4x^3)}{x}\log(x)\log(1-x) \\
+&\; \frac{(1+x)^2(5+7x^2-4x^3)}{x}\log(x)\log(1+x) - \frac{(1-x)^2(5+3x)(1+x+4x^2)}{x}\mathrm{Li}_2(x) \\
+&\; \frac{5+2x+12x^2+6x^3-x^4-4x^5}{x}\mathrm{Li}_2(-x) \Bigg],
\end{aligned} \tag{A7}$$

$$\begin{aligned}
\Gamma_b^- \;=&\; 4(1-x^2)^2 + \frac{\alpha_s}{4\pi} C_F \Bigg[\frac{4}{3}(1-x)(16-14x+22x^2+18x^3-3x^4-3x^5) \\
-&\; \frac{\pi^2}{3}4(4+x^4) + 8x^2(1+5x^2)\log(x) - 24(1-x^2)^2\log(1-x) + 8(1-x^2)(2-x^2)\log(1+x) \\
-&\; 4(1-x)^2(4+5x+6x^2+x^3)\log(x)\log(1-x) - 4(1+x)^2(4-5x+6x^2-x^3)\log(x)\log(1+x) \\
-&\; 4(1-x)^2(12+21x+14x^2+x^3)\mathrm{Li}_2(x) - 4(12+3x+6x^3-x^5)\mathrm{Li}_2(-x) + 8(1-x^2)^2\log\left(\frac{m_t^2}{\mu^2}\right) \Bigg],
\end{aligned} \tag{A8}$$

$$\begin{aligned}
\Gamma_{ab}^- \;=&\; 2(1-x^2)^2 + \frac{\alpha_s}{4\pi} C_F \Bigg[2(1-x)(9-6x+6x^2-5x^3) - \frac{2\pi^2}{3}(5+2x^4) + 2x^2(1+3x^2)\log(x) \\
-&\; \frac{2(1-x^2)^2(1+5x^2)}{x^2}\log(1-x) - \frac{2(1-x^2)(1-9x^2-2x^4)}{x^2}\log(1+x) \\
-&\; 2(1-x)^2(5+7x+4x^2)\log(x)\log(1-x) - 2(1+x)^2(5-7x+4x^2)\log(x)\log(1+x) \\
-&\; 2(1-x)^2(13+23x+12x^2)\mathrm{Li}_2(x) - 2(15+3x+5x^2+x^3+4x^4)\mathrm{Li}_2(-x) + 2(1-x^2)^2\log\left(\frac{m_t^2}{\mu^2}\right) \Bigg].
\end{aligned} \tag{A9}$$